## Partial synchronization patterns in brain networks

ECKEHARD SCHÖLL<sup>1,2,3</sup>

- <sup>1</sup> Institut für Theoretische Physik, Technische Universität Berlin, Hardenbergstraße 36, 10623 Berlin, Germany
- <sup>2</sup> Potsdam Institute for Climate Impact Research, Telegrafenberg A 31, 14473 Potsdam, Germany
- <sup>3</sup> Bernstein Center for Computational Neuroscience Berlin, Humboldt-Universität, 10115 Berlin, Germany

PACS 05.45.Xt – Synchronization; coupled oscillators PACS 87.19.1j – Neuronal network dynamics

Abstract —Partial synchronization patterns play an important role in the functioning of neuronal networks, both in pathological and in healthy states. They include chimera states, which consist of spatially coexisting domains of coherent (synchronized) and incoherent (desynchronized) dynamics, and other complex patterns. In this perspective article we show that partial synchronization scenarios are governed by a delicate interplay of local dynamics and network topology. Our focus is in particular on applications of brain dynamics like unihemispheric sleep and epileptic seizure.

Introduction. -Synchronization is a widespread natural phenomenon occurring in dynamical networks of nonlinear oscillators [1, 2]. Probably the first example was given by Christiaan Huygens (1629 - 1695), who observed that while two individual pendulum clocks show slightly deviating times, they spontaneously synchronize at exactly the same frequency if they are weakly coupled via a wooden beam. In the human brain, synchronization of neurons is essential for normal physiological functioning [3], for instance in the context of cognition and learning, but it is also strongly related to pathological conditions such as Parkinson's disease [4], or epileptic seizures, which are the cardinal symptom of epilepsy [5–7]. This neurological disease is currently understood as a network disease [8], and a better understanding of the role of the epileptic network's topology in seizure generation and termination is highly desirable. Sleep is associated with specific synchronized oscillations, i.e., sleep spindles and slow oscillations in the thalamocortical system [9]. While the synchronization processes can differ between adults and children [10], transitions from wakefulness to sleep are widely accompanied by synchronization phenomena [11]. A particularly intriguing phenomenon in nature is unihemispheric slow-wave sleep, exhibited by aquatic mammals including whales, dolphins and seals, and multiple bird species. Unihemispheric sleep, as the name suggests, is the remarkable ability to engage in deep (slow-wave) sleep with a single hemisphere of the brain while the other hemisphere remains awake [12–14]. Interestingly, sleep and wakefulness are characterized by a high and low degree of synchronization, respectively [12]. In the human brain the first-night effect, which describes troubled sleep in a novel environment, has been related to asymmetric dynamics recently, i.e., a manifestation of one hemisphere of the brain being more vigilant than the other [15].

Using complex networks of coupled oscillators, one can simulate synchronization phenomena observed in the human brain. Often coupled oscillators of FitzHugh-Nagumo type are employed since these are a paradigmatic model for neural dynamics [16]. The model describes the nonlinear dynamics of individual neurons or whole brain areas by a fast excitatory and a slow inhibitory variable. The coupling between different neurons or different areas of the brain is mediated by a coupling matrix, which may be mathematically constructed using standard procedures from network science, or taken from empirical structural brain connectivities of human subjects measured, e.g., by diffusion-weighted magnetic resonance imaging (MRI) [17]. The role of distant-dependent transmission time delays in large-scale brain synchronization has been stressed in [18].

In this perspective article we focus on partial synchronization patterns related to unihemispheric sleep and epileptic seizures. We review computer simulations of networks based upon empirical connectivities and FitzHugh-Nagumo dynamics on the nodes of the network, which sheds light on dynamical phenomena in the brain. In our first application, we find dynamical symmetry-breaking between the two hemispheres, and in a minimum model

discuss the modalities of unihemispheric sleep in human brain, where one hemisphere sleeps while the other remains awake [19]. In the second application, we observe spontaneously occurring episodes of strong synchronization, which resemble the ones seen during epileptic seizures recorded by electroencephalography (EEG) [20, 21]. For a better insight into the network properties giving rise to such pathological events, we simulate the dynamics on various artificial network topologies: we randomly rewire links in a small-world fashion, consider fractal connectivities, and exchange equal weights with empirical weights from diffusion-weighted magnetic resonance imaging. Moreover, we explore how global aspects of the networks - as assessed with the average clustering coefficient and the mean shortest path length – impact on the dynamics of the epileptic-seizure-related synchronization phenomena.

A better knowledge of the interplay between dynamics and network properties leading to complex synchronization phenomena is essential for understanding unihemispheric sleep and epileptic seizures, as well as other synchronization phenomena in the brain like full or partial relay synchronization between distant areas of the brain. The paradigm is to use simple nonlinear oscillator models like single-variable phase oscillators or two-variable activator-inhibitor models in combination with complex network structures obtained empirically or from artificially constructed topologies. This opens up promising perspectives for future research on partial synchronization patterns in the brain.

Partial synchronization patterns. - There exist different forms of synchronization, i.e., complete or isochronous (zero-lag) synchronization, generalized synchronization (where the oscillations of the individual elements of the network are not identical, but functionally related), phase synchronization (where only the phases but not the amplitudes of the oscillations are synchronized), frequency synchronization (where only the frequencies but not the phases are the same), cluster or group synchronization (where within each cluster all elements are completely synchronized, but between the clusters there is a phase lag), and many other forms. Some progress has been made in generalizing synchronization, for instance, towards adaptive networks [22, 23] (where the strength of the links is adapted dynamically), inhomogeneous local dynamics [24] and heterogeneous delay times [18], distributed, state-dependent, or time-varying delays.

Recent research interest has focussed on more complex partial synchronization patterns, where the whole system is not completely in synchrony, but only parts of it have the same phase and frequency. An intriguing example of partial synchronization patterns, which has recently gained much attention, are *chimera states*, i.e., symmetry-breaking states of partially coherent and partially incoherent behavior, for recent reviews see [25–27]. Chimera states in dynamical networks consist of spa-

tially separated, coexisting domains of synchronized (spatially coherent) and desynchronized (spatially incoherent) dynamics. They are a manifestation of spontaneous symmetry-breaking in systems of identical oscillators, and occur in a variety of physical, chemical, biological, neuronal, ecological, technological, or socio-economic systems. Other examples of partial synchronization include solitary states [28], or hierarchical multifrequency clusters [23].

In the following we model each node of the network, corresponding to a brain region, by the FitzHugh-Nagumo (FHN) model, a paradigmatic model for neuronal spiking [29, 30]. Note that while the FHN model is a simplified model of a single neuron, it is also often used as a generic model for excitable media on a coarse-grained level [31,32]. Thus the dynamics of the network reads:

$$\varepsilon \dot{u}_{k} = u_{k} - \frac{u_{k}^{3}}{3} - v_{k} 
+ \sigma \sum_{j \in N_{H}} A_{kj} \left[ B_{uu}(u_{j} - u_{k}) + B_{uv}(v_{j} - v_{k}) \right] \quad (1a) 
+ \varsigma \sum_{j \notin N_{H}} A_{kj} \left[ B_{uu}(u_{j} - u_{k}) + B_{uv}(v_{j} - v_{k}) \right] , 
\dot{v}_{k} = v_{k} + a 
+ \sigma \sum_{j \in N_{H}} A_{kj} \left[ B_{vu}(u_{j} - u_{k}) + B_{vv}(v_{j} - v_{k}) \right] \quad (1b) 
+ \varsigma \sum_{j \notin N_{H}} A_{kj} \left[ B_{vu}(u_{j} - u_{k}) + B_{vv}(v_{j} - v_{k}) \right] ,$$

with  $k \in N_{\rm H}$  where  $N_{\rm H}$  denotes either the set of nodes kbelonging to the left  $(N_L)$  or the right  $(N_R)$  hemisphere, and  $\varepsilon = 0.05$  describes the timescale separation between fast activator variable or neuron membrane potential uand the slow inhibitor or recovery variable v [29]. Depending on the threshold parameter a, the FHN model may exhibit excitable behavior (|a| > 1) or self-sustained oscillations (|a| < 1). Here we use the FHN model in the oscillatory regime and fix the threshold parameter at a = 0.5 sufficiently far from the Hopf bifurcation point. The coupling within the hemispheres is given by the intra-hemispheric coupling strength  $\sigma$  while the coupling between the hemispheres is given by the inter-hemispheric coupling strength ς. The interaction scheme between nodes is characterized by a rotational coupling matrix **B**. Employing a rotational matrix  $\mathbf{B}$  is a simple way to parameterize the possibility of either diagonal coupling  $(B_{uu}, B_{vv})$  or activator-inhibitor cross-coupling  $(B_{uv}, B_{vu})$  by a single parameter  $\varphi$ :

$$\mathbf{B} = \begin{pmatrix} B_{uu} & B_{uv} \\ B_{vu} & B_{vv} \end{pmatrix} = \begin{pmatrix} \cos\varphi & \sin\varphi \\ -\sin\varphi & \cos\varphi \end{pmatrix}. \tag{2}$$

In the following we choose  $\varphi = \frac{\pi}{2} - 0.1$ , causing dominant activator-inhibitor cross-coupling [33], which is a commonly employed mechanism in biology. In the neurosciences, the microscopic coupling schemes are very complex [34], but in our coarse-grained macroscopic description of a whole brain area by a pair of activator and inhibitor variables, activator-inhibitor coupling is a natural

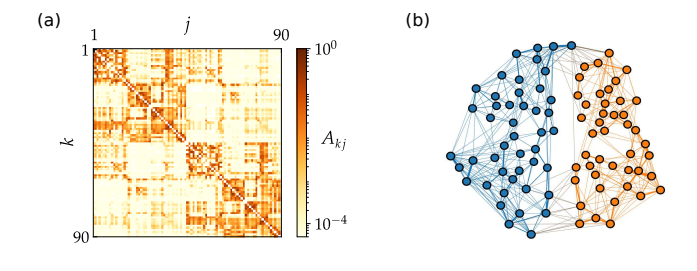


Fig. 1: Model for the hemispheric brain structure: (a) Weighted coupling matrix  $A_{kj}$  of the averaged empirical structural brain network derived from twenty healthy human subjects. The 90 brain regions k,j are taken from the Automated Anatomic Labeling atlas [39], labeled such that k=1,...,45 and k=46,...,90 correspond to the left and right hemisphere, respectively. (b) Schematic representation of the graph of the brain structure with highlighted left (dark blue) and right (light orange) hemisphere. After [19].

extension of pure activator-activator coupling. Mathematically, this means that signals of other neuronal areas are coupled via a coupling phase, which introduces a phase lag or time delay. The subtle interplay of excitatory and inhibitory interaction enables intermittent periods of either high or low synchronization. This is typical of the critical state at the edge of different dynamical regimes in which the brain operates [35, 36]. The coupling phase  $\varphi$  is similar to the phase-lag parameter of the paradigmatic Kuramoto phase oscillator model [37], which is widely used to describe synchronization phenomena in coupled oscillator networks. The coupling phase has been shown to be crucial for the modeling of chimera patterns in the Kuramoto model [38] and in the FHN model [33].

First, we consider an empirical structural brain network, obtained from diffusion-weighted MRI data measured in healthy human subjects. For details regarding the experimental setup, data acquisition and processing, see [40]. Obtaining such connectivity information using diffusion tractography is known to face a range of challenges [41]. The 90 brain areas of the Automated Anatomical Labeling (AAL) atlas [39] correspond to the 90 nodes of our network, and the connecting white-matter fibers between the areas correspond to the links. To eliminate individual variation, the matrices of 20 subjects were averaged over the coupling between two brain regions k and j, giving rise to the topology of Fig. 1(a), (b). Brain areas  $k \in N_L = \{1, 2, \dots, 45\}$  and  $k \in N_R = \{46, \dots, 90\}$  correspond to the left and right hemisphere, respectively, as in [19,21]. The structure of the brain hemispheres can be easily distinguished: In the adjacency matrix in Fig. 1(a), the connections within one hemisphere are much stronger than the connections between both hemispheres. In Fig. 1(b) the hemispheric brain structure is schematically shown. Note that there is a very slight structural asymmetry of the two brain hemispheres, related to the known asymmetries in localization of psychological functions, such as the prevalence of language functions in the left brain hemisphere in humans.

These empirical structural connectivities have been used in computer simulations of unihemispheric sleep [19], of epileptic seizure [20,21], and of the influence of sound on brain networks, i.e., synchronization patterns induced by the frequency of an external sound source [42].

**Methods.** – The dynamical behavior can be characterized by the mean phase velocity  $\omega_k = 2\pi M_k/\Delta T$  for each node k, where M complete rotations are realized during  $\Delta T$ . Further, we use the global Kuramoto order parameter r to measure the degree of synchronization of a network:

$$r(t) = \frac{1}{N} \left| \sum_{k=1}^{N} \exp[i\phi_k(t)] \right|, \tag{3}$$

utilizing an abstract dynamical phase  $\phi_k$  obtained from the standard geometric phase  $\phi_k(t) = \arctan(v_k/u_k)$  by a transformation which yields constant phase velocity  $\dot{\phi}_k$ . For an uncoupled FHN oscillator, the function  $t(\phi_k)$  is calculated numerically, assigning a value of time  $0 < t(\phi_k) <$ T for every value of the geometric phase, where T is the oscillation period. The dynamical phase is then defined as  $\phi_k = 2\pi t(\tilde{\phi}_k)/T$ , which yields  $\dot{\phi}_k = \text{const.}$  Only by using the dynamical phase  $\phi_k$ , rather than the geometrical phase  $\tilde{\phi}_k(t)$ , strong temporal fluctuations of r(t) due to the slow-fast time scales of inhibitor and activator are suppressed, and a change in r indeed reflects a change in the degree of synchronization. The Kuramoto order parameter may vary between 0 and 1, where r=1 corresponds to complete phase synchronization, small values characterize desynchronized states, and intermediate values correspond to partial synchronization.

One may introduce the hemispheric Kuramoto order parameters  $R_L(t)$  and  $R_R(t)$  characterizing the left and the right hemisphere, respectively, by restricting the summation in Eq. (3) to the respective hemisphere.

Unihemispheric sleep. — In this section we apply the FitzHugh-Nagumo model with the empirical structural connectivity introduced in the previous section to study the phenomenon of unihemispheric sleep [19]. We show that the dynamical asymmetry of the two brain hemispheres, induced by the slight natural structural asymmetry, can be enhanced by introducing the inter-hemispheric coupling strength as a control parameter for partial synchronization patterns. It has been speculated that unihemispheric sleep is related to the spontaneous symmetry-breaking phenomenon of chimera states in oscillator networks [43, 44].

It is presumed that a certain degree of structural interhemispheric separation is a necessary condition for this pattern to persist [12]. Therefore we propose to model unihemispheric sleep by a two-community network

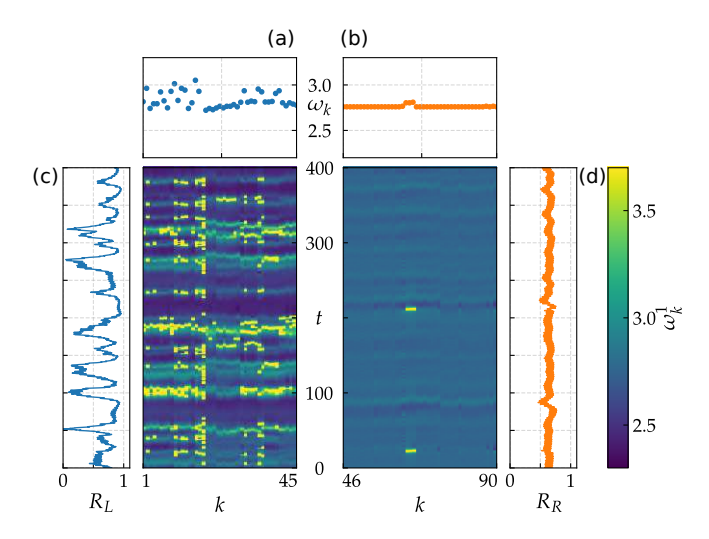


Fig. 2: (color online) Partial synchronization pattern for  $\sigma=0.70,\ \varsigma=0.15$  with low and high degree of synchronization in the left (a, c) and right (b, d) hemisphere, respectively. (a),(b) Mean phase velocity profiles  $\omega_k$ , averaged over  $\Delta T=5\,000$ . (c),(d) inner panels: space-time plots of node-wise phase velocity  $\omega_k^1$  averaged over a single oscillation, outer panels: hemispheric Kuramoto order parameter  $R_{L,R}$  as a function of time t. Parameters:  $\varepsilon=0.05,\ \alpha=0.5,\ \varphi=\frac{\pi}{2}-0.1$ . After [19].

of the two hemispheres where the inter-hemispheric coupling strength is smaller than the intra-hemispheric coupling. Similar results are expected if the longer propagation time delays between the two hemispheres are taken into account [18]. We consider the empirical structural brain network shown in Fig. 1, where each region of interest is modeled by a single FitzHugh-Nagumo oscillator Eq. (1). To achieve partial synchronization patterns we consider the inter-hemispheric coupling strength  $\varsigma$  as an independent parameter that allows us to reduce the coupling between the hemispheres. In a certain intermediate interval of inter-hemispheric coupling strength  $\varsigma < \sigma$  we find the partial synchronization pattern shown in Fig. 2 where the left hemisphere is incoherent while the right is frequency-synchronized, except for three small brain regions (hippocampus, gyrus parahippocampalis, and amygdala). Interestingly, these three special regions occasionally perform an extra oscillation thus leading occasionally to a higher instantaneous frequency, and within the network they have a pacemaker role. The partial synchronization shows up in the space-time plot, in the mean phase velocity profile, and in the hemispheric Kuramoto order parameter (although there is no perfect phase synchronization, and hence  $R_R < 1$ ). Note that the incoherent, left hemisphere occasionally exhibits a high degree of synchronization that, in contrast to the right hemisphere, is unstable and vanishes after a short while.

In conclusion, we have obtained a symmetry-broken state, where the (right) frequency-synchronized hemi-

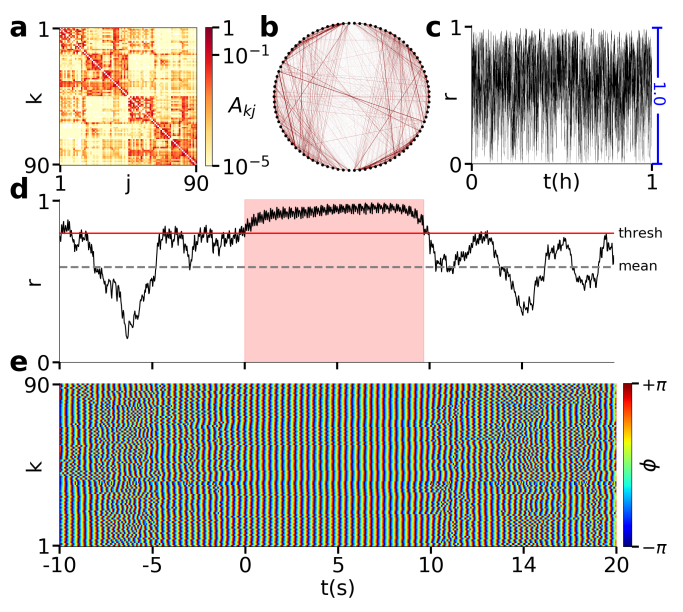


Fig. 3: Epileptic-seizure-like synchronization phenomena in a FitzHugh-Nagumo network with empirical connectivity. (a) Weighted adjacency matrix. (b) Schematic network structure, where the left (right) semicircle corresponds to the left (right) hemisphere (nodes are numbered clockwise sequentially 1,...,90 starting from the bottom of the circle). (c) Global Kuramoto order parameter r vs time for a time interval of 1 hour. (d) r vs time for a time interval of 30 seconds. The horizontal dashed grey line denotes the time average  $\langle r \rangle$  over 3 hours. The horizontal full red line marks the threshold of r = 0.8. If r > 0.8 for more than 8 seconds, we define this as a seizure (pink shaded region). (e) Space-time plot of the dynamical phases corresponding to panel (d). The left (right) hemisphere is shown in the lower (upper) half. Simulation parameters:  $\varepsilon = 0.05, \ a = 0.5, \ \varphi = \frac{\pi}{2} - 0.1, \ N = 90, \ \sigma = \varsigma = 0.6.$ After [21].

sphere is reminiscent of the sleep state, and the (left) desynchronized hemisphere ressembles an awake state.

Epileptic-seizure-related synchronization phenomena. — Epilepsy is a neurological disorder that affects almost 70 million people worldwide. In epileptology, the development of the concept of an epileptic network [45, 46] received a strong impetus from network-theoretical concepts. An epileptic network comprises anatomically, and more importantly, functionally connected cortical and subcortical brain structures and regions. Seizures may emerge from network constituents that generate and sustain normal, physiological brain dynamics during the seizure-free interval [45].

For networks of neurons, modeled with the FitzHugh-Nagumo neuronal dynamics, epileptic-seizure-like dynamics has previously been investigated in an empirical structural brain connectivity and a mathematically constructed network with modular fractal connectivity [20]. Further,

the role of partial synchronization phenomena for mechanisms of seizure initiation [47] and termination [48] has been explored. Here we present the results of simulations for different network topologies that shed light on the role of the coupling structure for spontaneous synchronization [21].

First we use the FHN model Eq.(1) with the empirical structural brain network of Fig. 1. The coupling strength  $\sigma = \varsigma$  is chosen such that it is as high as possible while still avoiding full synchronization for long simulations ( $\approx$  10000 time units), i.e.,  $\sigma = 0.6$ . In order to compare our simulations with real data (EEG recordings of absence seizures), we transform the dimensionless time units of the FHN oscillator model to real time units by comparing the oscillation period of a single FHN oscillator T = 2.56 to the dominant frequency of an absence seizure at about f = 3Hz [49]. Therefore, the simulation time is converted to real time by  $1s = 2.56 \cdot 3 = 7.68$  simulation time units.

The results of the simulation are shown in Fig. 3. In panels (c) and (d), we show the global Kuramoto order parameter r(t), which measures the degree of synchronization. Panels (c) and (d) also reveal periods of very high and of very low synchronization of the system as a function of time, varying in a range from 0 to almost 1 (panel (c)). The temporal average of the order parameter  $\langle r \rangle$  (horizontal dashed grey line in (d)) and its standard deviation  $\delta$  are given by  $\langle r \rangle \pm \delta = 0.59 \pm 0.21$  for the full simulation of 164 minutes. We define a threshold of high synchrony as  $r_{\rm th} = \langle r \rangle + \delta = 0.8$  (horizontal red line in (d)). In the simulation presented in Fig. 3, the order parameter is found to be in high synchrony with r > 0.8 during 17% of the simulation time. Only if the synchronization remains above the threshold for at least 8 seconds, we define this time interval as a seizure.

In Fig. 3(d), the order parameter is shown versus time for one exemplary seizure. Approximately 6 seconds prior to the start of the seizure, the order parameter drops to a low value of  $r\approx 0.2$ . Such an apparent desynchronization can often be observed prior to the onset of focal epileptic seizures [47,50–52]. The order parameter then increases above r>0.8 (onset of seizure) and remains in high synchrony for almost 10 seconds. The seizure interval is shown as a pink shaded region. In the full simulation of 164 minutes, 11 seizures were detected, giving an average of 4 seizures per hour and an average duration of 11 seconds. In Fig. 3(e), the dynamic phases of the oscillators are shown as space-time plot for the same time interval as in (d) exhibiting strong synchronization during seizure.

We have compared the simulations with EEG recordings from a 12 years old subject who suffered from seizures, and found good agreement of the simulated and the recorded seizures (see Supplemental Material).

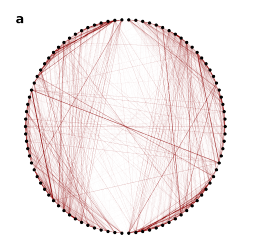
Empirical vs artificially constructed networks. — In order to gain deeper insight into the interplay of dynamics and network topology, especially regarding the occurrence of seizures, different artificially constructed networks

have been considered [21]. For details see the Supplemental Material

First, by randomly rewiring its links, the highly organized structure of the empirical connectivity matrix can be artificially destroyed, while keeping the weight distribution and average node strength. On average the system is less synchronized, and no seizure is found in the simulation. Next, a quasi-fractal connectivity on a ring network is considered. It synchronizes completely at a relatively small coupling strength  $\sigma$ , and no clearly defined seizures are found. To achieve a more realistic weight distribution, all non-zero links of the fractal ring can be replaced by randomly chosen weights of the empirical connectivity matrix in Fig. 1(a). However, despite rich, brain-like modulated synchronization behavior with a few very short events of high synchrony r > 0.8, not a single well-defined seizure is detected.

Finally, we consider small-world-like networks, which can be constructed according to the Watts-Strogatz algorithm [53] by starting from a nonlocally coupled ring and randomly rewiring links with a probability p. The impact of the average clustering coefficient and the average shortest path length on the number of observed epileptic-seizure-related synchronization episodes is evaluated. Intuitively, the clustering coefficient of the network measures the probability of "cliques" in the network: using the language of social networks, a "clique" is a group of people who are all connected with each other within this clique, i.e., if A has two friends, then these two are also friends with each other. Analogously, a network has a large clustering coefficient if whenever an element is connected to two other elements (open triplet), then these two are also likely to be connected directly (closed triplet). We have examined both network measures, clustering coefficient and shortest path length, by employing the Watts-Strogatz small-world algorithm with various rewiring probabilities p. Among the artificial networks, a small-world network with intermediate rewiring probability  $p \approx 0.232$  results in the best agreement with the simulations for empirical structural connectivity. For the other network topologies, either no spontaneously occurring epileptic-seizure-related synchronization phenomena are found in the simulated dynamics, or the overall degree of synchronization remains high throughout the simulation. This indicates that a topology with some balance of regularity and randomness favors the self-initiation and self-termination of episodes of high, seizure-like synchronization. In particular, the value of the clustering coefficient should not be too high (as for regular ring networks, p = 0) and not too low (as for pure random networks, p=1), and thus the rewiring probability should assume intermediate values between 0 and 1. Random network structures increase brain synchronization compared to realistic brain networks. There is a subtle interplay of regularity and randomness.

In conclusion, our simulations indicate that the human brain seems to effectively function in a specific window



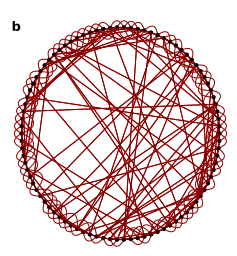


Fig. 4: Comparison of (a) empirical brain network, (b) artificial brain network (small world with rewiring probability p=0.232, clustering coefficient C=0.25). Each black dot represents one of 90 brain areas; the left (right) semicircle corresponds to the left (right) hemisphere.

of medium clustering. If the clustering is too large, the neural synchronization is approximately constant in time. The brain, however, shows both low and high synchronization values on the EEG during different tasks and mental states such as sleep. Moreover, epileptic brains, which function normally most of the time, appear to synchronize during seizures fully. This shows that the brain is capable of sustaining both very coherent and very incoherent oscillatory states, which is not possible for too large clustering coefficients. On the other hand, if the clustering coefficient is too small, the synchronization fluctuates rapidly in time and does not resemble the dynamics of simulations with an empirical brain network. One might speculate, based on these simulations, that the difference between healthy and epileptic brains might show up in the network's slightly altered clustering coefficient [54,55].

Conclusions and future challenges. – Partial synchronization patterns play an essential role in collective brain dynamics. Computer simulations of dynamical networks of nonlinear oscillators can help to understand the functioning of the brain, both in pathological and in healthy states. It is known that the brain is operating in a critical state at the edge of different dynamical regimes [35, 36]. We have shown that simple oscillator models in combination with complex network structures can explain and elucidate a plethora of observed partial synchronization scenarios, which are governed by a delicate interplay of local dynamics and network topology. Using empirical structural network connectivities obtained from diffusion-weighted magnetic resonance imaging of humans together with paradigmatic dynamics, e.g. the FitzHugh-Nagumo model, on the nodes of the network, vields realistic scenarios of partial synchronization. They include chimera states, which consist of spatially coexisting domains of coherent (synchronized) and incoherent (desynchronized) dynamics, and other complex patterns.

First, we have focussed on unihemispheric sleep, where one hemisphere of the brain sleeps while the other remains awake. By tuning the coupling between the hemispheres we have shown that at intermediate inter-hemispheric coupling one hemisphere becomes incoherent, giving rise to a chimera-like partial synchronization pattern.

Second, we have shown that FitzHugh-Nagumo oscillators, coupled via empirical structural connectivities measured in human subjects, exhibit episodes of high synchronization that resemble the ones seen during epileptic seizures. Comparing our long-term simulations to EEG-recorded epileptic seizures, the simulations show striking similarities to the real data.

In order to gain more insight into the nature of the empirical structural connectivities of the brain, and into the interplay of dynamics and network topology, we have also studied different artificially constructed complex network structures, ranging from random networks, regular nonlocally coupled ring networks, ring networks with fractal connectivities, and small-world networks with various rewiring probabilities. Although at first glance the network structure of the empirical connectivities (Fig. 4a) and the small world network with rewiring probability p = 0.232 (Fig. 4b) do not at all look similar, the partial synchronization scenarios are found to be very similar, giving the best match among all artificial structures studied. This has been attributed to the intermediate value of the average clustering coefficient, which results in a sophisticated balance of synchrony and asynchrony with wide temporal variability.

We have discussed in detail unihemispheric sleep and epileptic seizures as examples of brain dynamics, but a great wealth of other collective dynamical behavior in the brain is amenable to this approach. For instance, in neuroscience various scenarios have been uncovered where specific brain areas, e.g., thalamus or hippocampus, act as a functional relay between other brain regions, having a strong influence on signal propagation, brain functionality, and dysfunctions [56–58]. Relay synchronization scenarios between remote layers of a network have been studied for three-layer networks with regular nonlocally coupled ring topology [26], randomly diluted small-world topologies, and configurations where the relay is a single node, i.e., a hub. Future promising perspectives of the research on relay functions in the brain should also use empirical connectivities.

\* \* \*

This work was supported by the Deutsche Forschungs-gemeinschaft (DFG, German Research Foundation) - Project Nos. 163436311 - SFB 910, 429685422, 440145547, and 308748074. I am grateful to R. Andrzejak, R. Berner, T. Chouzouris, J.C. Claussen, J. Czech, F. Drauschke, J. Hlinka, P. Jiruska, J. Koulen, K. Lehnertz, M. Mykietyshyn, I Omelchenko, L. Ramlow, A. Provata, G. Ruzzene, J. Sawicki, A. Škoch, G. Strelkova, S. Yanchuk, and A. Zakharova for stimulating collaborations.

## REFERENCES

- [1] A. Pikovsky, M. Rosenblum, and J. Kurths, Synchronization: a universal concept in nonlinear sciences, 1st ed. (Cambridge University Press, Cambridge, 2001).
- [2] S. Boccaletti, A. N. Pisarchik, C. I. del Genio, and A. Amann, Synchronization: From Coupled Systems to Complex Networks (Cambridge University Press, 2018).
- [3] W. Singer, Eur. J. Neurosci. 48, 2389 (2018).
- [4] P. A. Tass, M. Rosenblum, J. Weule, J. Kurths, A. Pikovsky, J. Volkmann, A. Schnitzler, and H. J. Freund, Phys. Rev. Lett. 81, 3291 (1998).
- [5] K. Lehnertz, S. Bialonski, M.-T. Horstmann, D. Krug, A. Rothkegel, M. Staniek, and T. Wagner, J. Neurosci. Methods 183, 42 (2009).
- [6] P. Jiruska, M. de Curtis, J. G. R. Jefferys, C. A. Schevon, S. J. Schiff, and K. Schindler, J. Physiol. 591.4, 787 (2013).
- [7] V. K. Jirsa, W. C. Stacey, P. P. Quilichini, A. I. Ivanov, and C. Bernard, Brain 137, 2210 (2014).
- [8] K. Lehnertz, G. Ansmann, S. Bialonski, H. Dickten, C. Geier, and S. Porz, Physica D 267, 7 (2014).
- [9] M. Steriade, D. A. McCormick, and T. J. Sejnowski, Science 262, 679 (1993).
- [10] M. Spiess, G. Bernardi, S. Kurth, M. Ringli, F. M. Wehrle, O. G. Jenni, R. Huber, and F. Siclari, Neuroimage 178, 23 (2018).
- [11] F. Moroni, L. Nobili, F. De Carli, M. Massimini, S. Francione, C. Marzano, P. Proserpio, C. Cipolli, L. De Gennaro, and M. Ferrara, Neuroimage 60, 497 (2012).
- [12] N. C. Rattenborg, C. J. Amlaner, and S. L. Lima, Neurosci. Biobehav. Rev. 24, 817 (2000).
- [13] N. C. Rattenborg, B. Voirin, S. M. Cruz, R. Tisdale, G. Dell'Omo, H. P. Lipp, M. Wikelski, and A. L. Vyssotski, Nat. Commun. 7, 12468 (2016).
- [14] G. G. Mascetti, Nat Sci Sleep 8, 221 (2016).
- [15] M. Tamaki, J. W. Bang, T. Watanabe, and Y. Sasaki, Curr. Biol. 26, 1190 (2016).
- [16] D. S. Bassett, P. Zurn, and J. I. Gold, Nat. Rev. Neurosci. 19, 566 (2018).
- [17] P. Sanz-Leon, S. A. Knock, A. Spiegler, and V. K. Jirsa, Neuroimage 111, 385 (2015).
- [18] S. Petkoski and V. K. Jirsa, Phil. Trans. R. Soc. A 377, 20180132 (2019).
- [19] L. Ramlow, J. Sawicki, A. Zakharova, J. Hlinka, J. C. Claussen, and E. Schöll, EPL 126, 50007 (2019).
- [20] T. Chouzouris, I. Omelchenko, A. Zakharova, J. Hlinka, P. Jiruska, and E. Schöll, Chaos 28, 045112 (2018).
- [21] M. Gerster, R. Berner, J. Sawicki, A. Zakharova, A. Skoch, J. Hlinka, K. Lehnertz, and E. Schöll, Chaos 30, 123130 (2020).
- [22] D. V. Kasatkin, S. Yanchuk, E. Schöll, and V. I. Nekorkin, Phys. Rev. E 96, 062211 (2017).
- [23] R. Berner, Patterns of Synchrony in Complex Networks of Adaptively Coupled Oscillators (Springer, Cham, 2021).
- [24] F. Sorrentino and L. M. Pecora, Chaos 26, 094823 (2016).
- [25] E. Schöll, Nova Acta Leopoldina **425**, 67 (2020).
- [26] J. Sawicki, Delay controlled partial synchronization in complex networks (Springer, Heidelberg, 2019).
- [27] A. Zakharova, Chimera Patterns in Networks: Interplay between Dynamics, Structure, Noise, and Delay, Understanding Complex Systems (Springer, Cham, 2020).

- [28] Y. Maistrenko, B. Penkovsky, and M. Rosenblum, Phys. Rev. E 89, 060901 (2014).
- [29] R. FitzHugh, Biophys. J. 1, 445 (1961).
- [30] J. Nagumo, S. Arimoto, and S. Yoshizawa., Proc. IRE 50, 2061 (1962).
- [31] A. Chernihovskyi, F. Mormann, M. Müller, C. E. Elger, G. Baier, and K. Lehnertz, J. Clin. Neurophysiol. 22, 314 (2005).
- [32] A. Chernihovskyi and K. Lehnertz, Int. J. Bifurc. Chaos 17, 3425 (2007).
- [33] I. Omelchenko, O. E. Omel'chenko, P. Hövel, and E. Schöll, Phys. Rev. Lett. 110, 224101 (2013).
- [34] A. E. Pereda, Nat. Rev. Neurosci. 15, 250 (2014).
- [35] P. Massobrio, L. de Arcangelis, V. Pasquale, H. J. Jensen, and D. Plenz, Front. Syst. Neurosci. 9, 22 (2015).
- [36] J. Shi, K. Kirihara, M. Tada, M. Fujioka, K. Usui, D. Koshiyama, T. Araki, L. Chen, K. Kasai, and K. Aihara, Front. Netw. Physiol. (2021), to be published.
- [37] Y. Kuramoto, Chemical Oscillations, Waves and Turbulence (Springer-Verlag, Berlin, 1984).
- [38] O. E. Omel'chenko, M. Wolfrum, and Y. Maistrenko, Phys. Rev. E 81, 065201(R) (2010).
- [39] N. Tzourio-Mazoyer, B. Landeau, D. Papathanassiou, F. Crivello, O. Etard, N. Delcroix, B. Mazoyer, and M. Joliot, Neuroimage 15, 273 (2002).
- [40] T. Melicher, J. Horacek, J. Hlinka, F. Spaniel, J. Tintera, I. Ibrahim, P. Mikolas, T. Novak, P. Mohr, and C. Hoschl, Schizophr. Res. 162, 22 (2015).
- [41] J. Hlinka and S. Coombes, European Journal of Neuroscience 36, 2137 (2012).
- [42] J. Sawicki and E. Schöll, Front. Appl. Math. Stat. 7, 662221 (2021).
- [43] D. M. Abrams, R. E. Mirollo, S. H. Strogatz, and D. A. Wiley, Phys. Rev. Lett. 101, 084103 (2008).
- [44] A. E. Motter, Nat. Phys. 6, 164 (2010).
- [45] S. S. Spencer, Epilepsia 43, 219 (2002).
- [46] L. Kuhlmann, K. Lehnertz, M. P. Richardson, B. Schelter, and H. P. Zaveri, Nat. Rev. Neurol. 14, 618 (2018).
- [47] R. G. Andrzejak, C. Rummel, F. Mormann, and K. Schindler, Sci. Rep. 6, 23000 (2016).
- [48] A. Rothkegel and K. Lehnertz, New J. Phys. 16, 055006 (2014).
- [49] L. Sadleir, K. Farrell, S. Smith, M. Connolly, and I. Scheffer, Neurology 67, 413 (2006).
- [50] F. Mormann, K. Lehnertz, P. David, and C. E. Elger, Physica D 144, 358 (2000).
- [51] F. Mormann, T. Kreuz, R. G. Andrzejak, P. David, K. Lehnertz, and C. E. Elger, Epilepsy Res. 53, 173 (2003).
- [52] S. Feldt, H. Osterhage, F. Mormann, K. Lehnertz, and M. Zochowski, Phys. Rev. E 76, 021920 (2007).
- [53] D. J. Watts and S. H. Strogatz, Nature 393, 440 (1998).
- [54] M.-T. Horstmann, S. Bialonski, N. Noennig, H. Mai, J. Prusseit, J. Wellmer, H. Hinrichs, and K. Lehnertz, Clin. Neurophysiol. 121, 172 (2010).
- [55] G. Ansmann and K. Lehnertz, J. Neurosci. Methods 208, 165 (2012).
- [56] P. Roelfsema, A. Engel, P. König, and W. Singer, Nature 385, 157 (1997).
- [57] S. M. Sherman, Nat. Neurosci. 19, 533 (2016).
- [58] L. L. Gollo, C. R. Mirasso, M. Atienza, M. Crespo-Garcia, and J. L. Cantero, PLoS ONE 6, e17756 (2011).